Published in final edited form as:
Nucl Med Biol. 2008 August ; 35(6): 713–720. doi:10.1016/j.nucmedbio.2008.06.001.

Autoradiographic and Small-Animal PET Comparisons Between ^{18}F-FMISO, ^{18}F-FDG, ^{18}F-FLT and the Hypoxic Selective ^{64}Cu-ATSM in a Rodent Model of Cancer

Carmen S. Dence, **Datta E. Ponde**, **Michael J. Welch**, and **Jason S. Lewis**[*,#]
Mallinckrodt Institute of Radiology, the Alvin J. Siteman Cancer Center, Washington University School of Medicine, 510 S. Kingshighway Blvd., St. Louis, MO 63110, USA.

Abstract

Introduction—Cu-ATSM, a hypoxia imaging agent, has been shown to be predictive of response to traditional cancer therapies in patients with a wide range of tumors. It is known that the environment of the tumor results in a myriad of physiological consequences, including hypoxia, alterations in metabolism and proliferation. In an effort to better characterize the relationships between Cu-ATSM and other prominent radiopharmaceuticals, this current study was undertaken to compare the regional distribution of ^{64}Cu-ATSM with ^{18}F-FMISO, ^{18}F-FDG and ^{18}F-FLT in 9L tumors.

Methods—Taking advantage of the different half-life of ^{18}F ($t_{½}$ = 110 min) in comparison to ^{64}Cu ($t_{½}$ = 12.7 h), we undertook a dual tracer autoradiography study in 9L tumors. Four groups were examined: (a) ^{18}F-FMISO, 2 h p.i. and ^{64}Cu-ATSM 10 min p.i. (b) ^{18}F-FMISO, 2 h p.i. and ^{64}Cu-ATSM 24 h p.i. (c) ^{18}F-FDG, 1 h p.i. and ^{64}Cu-ATSM 10 min p.i., and (d) ^{18}F-FLT, 1 h p.i. and ^{64}Cu-ATSM 10 min p.i.. Small animal PET imaging was performed in 9L tumor-bearing rats with imaging on concurrent days comparing ^{64}Cu-ATSM with ^{18}F-FMISO and ^{18}F-FLT.

Results—It was shown that the regional distribution of ^{18}F-FMISO and ^{64}Cu-ATSM showed an excellent correlation when the ^{64}Cu-ATSM had been allowed to distribute for either 10 min (R^2 = 0.84) or 24 h (R^2 = 0.86). The regional comparisons between ^{64}Cu-ATSM (10 min) and ^{18}F-FDG (1 h) resulted in a very poor correlation (R^2 = 0.08) between the regional uptake of the two agents. The comparison between ^{18}F-FLT and ^{64}Cu-ATSM showed a strong relationship (R^2 = 0.83) between the two tracers. The small-animal PET images for the distribution comparisons between ^{64}Cu-ATSM and ^{18}F-FMISO and ^{18}F-FLT were in agreement with the data generated from the autoradiography studies.

Conclusions—The data show that it is important to remember that a number of different metabolic situations can exist when considering the relationship between regions of high glucose uptake, proliferation and hypoxia.

Keywords

hypoxia; proliferation; metabolism

Address all correspondence and requests for reprints to: Jason S. Lewis, Ph.D., Department of Radiology, Memorial Sloan-Kettering Cancer Center, 1275 York Avenue, New York, New York 10065, Tel: (646) 888-3038, Fax: (646) 422 0408, Email: lewisj2@mskcc.org.
[#]*Current affiliation:* Department of Radiology, Memorial Sloan-Kettering Cancer Center, New York, NY.

1. Introduction

The non-invasive imaging of hypoxia is of significant importance, given that the onset of hypoxia in malignant tissues is associated with and influenced by a myriad of complicated physiological processes [1–5]. Copper(II)-diacetyl-bis(N^4-methylthiosemicarbazone), or Cu-ATSM, is a hypoxia imaging agent that shows rapid delineation of tumor hypoxia (< 1 hour) in high tumor to background tissue ratios (tumor to blood ratios ≫ 2.0) [6,7]. In clinical studies Cu-ATSM has been shown to be predictive of response to traditional cancer therapies in patients with rectal, lung, and uterine cervix cancer [8–11]. In these same studies concurrent imaging with [^{18}F]fluoro-2-deoxy-D-glucose (^{18}F-FDG) showed no predictive value.

It is obvious that the macroenvironment of the tumor results in a wide range of physiological consequences, including hypoxia, alterations in metabolism and proliferation. An understanding of the relationships among these complicated interactions is of importance to both the basic scientist and the clinician. The relationship between hypoxia, proliferation and metabolism has partly been explored in clinical studies. A comparison between ^{18}F-fluoromisonidazole (^{18}F-FMISO) and ^{18}F-FDG uptake in humans demonstrated that some hypoxic tumors can have modest glucose metabolism, whereas some highly metabolic tumors are not hypoxic, showing discordance in tracer uptake that was tumor type specific [12]. ^{18}F-FDG uptake has been shown to correlate with tumor proliferative rates in lymphomas [13] and NSCLC [14]. However, Buck *et al* showed that ^{18}F-fluorothymidine (^{18}F-FLT) correlated significantly better with the proliferative activity of lung tumors than did ^{18}F-FDG [15].

In an effort to better characterize the relationships between Cu-ATSM and other validated radiopharmaceuticals, this study was undertaken to compare the regional distribution of ^{64}Cu-ATSM with ^{18}F-FDG (metabolism) and ^{18}F-FLT (proliferation). A comparison was also performed with ^{18}F-FMISO, given that the retention mechanisms for these two hypoxia tracers are different. By exploitation of the different half lives of ^{18}F ($t_{½}$ = 110 min) and ^{64}Cu ($t_{½}$ = 12.7 h), we undertook a dual tracer autoradiography study in a simple model of cancer, the 9L gliosarcoma model, in order to better understand the regional distribution of each tracer in comparison to each other.

2. Material and Methods

2.1. Materials

Unless otherwise stated, all chemicals were purchased from Aldrich Chemical Company, Inc. (Milwaukee, WI). All solutions were prepared using distilled, deionized water (Milli-Q®; >18 MΩ resistivity). High specific activity ^{64}Cu was produced on a CS-15 biomedical cyclotron at Washington University School of Medicine via published methods. ^{64}Cu-ATSM was synthesized by methods previously described [16], and ^{18}F-FMISO was synthesized according to procedures by McCarthy, Dence and Welch [17]. ^{18}F-FLT was produced by a modified version of Machulla et al [18]. All radiopharmaceuticals were used in >98 % radiochemical purity, as determined by radio-TLC and radio-HPLC.

2.2. Animal Models

All animal experiments were conducted in compliance with the Guidelines for the Care and Use of Research Animals established by Washington University's Animal Studies Committee. The 9L cells were a generous gift from the Brain Tumor Research Center, University of California (San Francisco). All studies were performed on 150–165 g female Fisher 344 rats (Charles River Laboratories, Wilmington MA). The Fischer rats were implanted subcutaneously with 1×10^7 9L gliosarcoma cells in the right flank and were used at day 14 of tumor growth. On the day of study the tumors were approximately 1.5 – 2 g, and on

postmortem examination had varying degrees of necrosis. In all cases, rats were anesthetized with 1–2% isoflurane (with room air) for administration of radiopharmaceuticals.

2.3. Dual Tracer Ex vivo Autoradiography

All electronic autoradiography was performed on an InstantImager Electronic Autoradiography System from Packard Instrument Co. (Meriden, CT). Four groups of 9L-bearing animals (n = 5 each group) were examined, in order to compare the regional distributions of the fluorinated tracers ^{18}F-FMISO, ^{18}F-FLT and ^{18}F-FDG. The four groups were (a) ^{18}F-FMISO, 2 h post injection and ^{64}Cu-ATSM 10 min post injection (b) ^{18}F-FMISO, 2 h post injection and ^{64}Cu-ATSM 24 h post injection (c) ^{18}F-FDG, 1 h post injection and ^{64}Cu-ATSM 10 min post injection, and (d) ^{18}F-FLT, 1 h post injection and ^{64}Cu-ATSM 10 min post injection. All rats received an i.v. injection of 1.0 – 1.2 mCi of the required ^{18}F tracer, followed by ^{64}Cu-ATSM. The administration of 50 – 60 μCi of ^{64}Cu-ATSM occurred after 110 min for (a) and 50 min after for (c) and (d). For (b), each rat (n = 5) received an i.v. injection of 240 μCi of ^{64}Cu-ATSM, followed 22 h later by ^{18}F-FMISO. After euthanasia, the tumors were excised and frozen whole in Miles, Inc., Tissue-Tek Embedding Medium (Elkhart, IN). Slices (1 mm thick) were mounted and placed in the InstantImager® in order to visualize the distribution of radioactivity. The slices were not washed at any time and were not treated with any preservative. Autoradiography of the slices initially visualized the ^{18}F localization (1 or 2 h distribution) and was repeated 24 h later, in order to visualize the ^{64}Cu-ATSM (10 min or 24 h distribution). Standard radioisotopic mixtures were also made and imaged in order to ensure that >95% of the initial image was generated by the ^{18}F and that only ^{64}Cu activity remained in the 24-h images.

To generate a comparison between the focal uptake of ^{64}Cu-ATSM and the ^{18}F-agents, a ‘template’ was generated from the ^{18}F image by use of the equipment software to yield the net % max uptake in each defined region. Briefly, the template generated by the software consists of an x–y grid that contains regions of interest (ROI’s) that have been determined by threshold levels defined automatically. The system uses three user-specified parameters to locate and create regions of interest based on separation, sensitivity and background. As a control in this study, regions of interest were also defined manually. The manual operation was performed where every individual tumor slice was first analyzed for the absolute number of counts. The ROIs based on separation were defined as percentages of the overall number of counts within the tumor ROI that showed the highest concentration of activity with fixed levels of sensitivity and background for individual slices. For both the manual and automatic analysis of the autoradiographs, identical templates and data were obtained.

The template generated for each ^{18}F image was overlaid on the complementary ^{64}Cu-ATSM image (i.e., the same tumor slice after ^{18}F decay) in order to generate the ^{64}Cu distribution data. As a control, a template was also generated on the ^{64}Cu image and then overlaid on the complementary ^{18}F image to generate the ^{18}F distribution data. The data presented (net % max) are defined as [a/b ×100 %], where a = number of counts/mm^2 in a defined ROI within a tumor slice and b = number of counts/mm^2 in the ROI with the highest number of counts from the same tumor slice. These analyses were performed on 10 tumor slices for each study group. Each tumor slice had at least 10 ROIs defined within its boundaries.

2.4. Small-Animal PET Comparisons

All small-animal PET imaging was undertaken on the microPET-Focus 220 [19] (Concorde MicroSystems Inc., Knoxville, TN) and were coregistered with CT images from a MicroCAT II System (ImTek Inc., Knoxville, TN). Isoflurane (1–2%) was used as an inhaled anesthetic to induce and maintain anesthesia during imaging. Drugs were administered via the tail vein. Two separate studies were performed in 9L bearing rats (n = 4 per group). (A) On Day 1, 150

μCi of ^{64}Cu-ATSM were injected into the animals and imaged 10 min post-injection. The animals were allowed to waken and on Day 2 (28 hours after ^{64}Cu-ATSM) were injected with 1.5 mCi ^{18}F-FMISO and imaged at 2 h post-injection; (B) On Day 1, 150 μCi of ^{64}Cu-ATSM were injected into the animals and imaged 10 min post-injection. The animals were allowed to waken and on Day 2 (28 hours after ^{64}Cu-ATSM) were injected with 1.5 mCi ^{18}F-FLT and imaged at 1 h post-injection. All PET scans consisted of a single static 5-min collection. The image registration between CT and PET images was accomplished by using a landmark registration technique, AMIRA image display software (AMIRA, TGS Inc, San Diego, CA). The registration method proceeds by rigid transformation of the microCT images from landmarks provided by fiducial markers directly attached to the animal bed.

3. Results

3.1. Dual Tracer Ex vivo Autoradiography

Shown in Figure 1A and 1B are representative sample slices from the autoradiographic studies comparing distribution of ^{18}F-FMISO (2 h) and ^{64}Cu-ATSM (10 min or 24 h). Figures 2A and 2B demonstrate the correlation of the regional uptake of ^{64}Cu at both time points with the 2-h distribution of ^{18}F-FMISO. It is evident, both through visual analysis and quantitative comparison, that the regional distributions of ^{18}F-FMISO and ^{64}Cu-ATSM show an excellent correlation when the ^{64}Cu-ATSM has been allowed to distribute for either 10 min ($R^2 = 0.84$) or 24 h ($R^2 = 0.86$). It is also evident from Figure 1B that Cu-ATSM at 24-h results in a more intense uptake within small discreet regions of the tumor volume, more so than is seen with the corresponding ^{18}F-FMISO image.

Figure 1C shows the regional comparisons between ^{64}Cu-ATSM (10 min) and ^{18}F-FDG (1 h). Visually, it appears that there are regions within the tumor with uptake similar for both tracers but also regions in which there is a complete discrepancy of uptake, where uptake of Cu-ATSM is not mirrored by uptake of ^{18}F-FDG. The quantitative analysis of these images (Figure 2C) confirms this, as demonstrated by a poor correlation ($R^2 = 0.08$) between the regional uptake of the two agents. The uptake of ^{18}F-FLT and ^{64}Cu-ATSM appear visually identical (Figure 1D), which is confirmed by quantitative analysis ($R^2 = 0.83$) (Figure 2D).

3.2. Small-Animal PET Comparisons

The small-animal PET images for the distribution comparisons between ^{64}Cu-ATSM and ^{18}F-FMISO and ^{18}F-FLT are given in Figure 3A and 3B, respectively. As with the autoradiography studies, similarities in regional uptake are noted between the two tracers even after 10 min of Cu-ATSM distribution. The images comparing ^{64}Cu-ATSM and ^{18}F-FLT are also in agreement with the data generated from the autoradiography studies. The intense uptake of tracers is on the tumor edge (the tumor had a histologically confirmed necrotic center).

4. Discussion

4.1. Regional Uptake of ^{64}Cu-ATSM and ^{18}F-FMISO Show a Strong Correlation

One of the most popular agents for the PET imaging of hypoxia has been ^{18}F-FMISO [12,20, 21]. Although Cu-ATSM has been validated for use *in vitro* and *in vivo* in multiple tumor models [6] and it is a very effective PET agent for clinically delineating many hypoxic human malignancies [8–11], there has been a concern that its ability to delineate hypoxia may be tumor-dependent. In 2005, it was shown *in vitro* that the hypoxia-selectivity of ^{64}Cu-ATSM was found to be cell line dependent. It was demonstrated that there was variation in the ^{64}Cu cellular accumulation, with uptake in normoxic cells being anywhere from two to nine times lower than that in hypoxic cells, depending upon the cell line [22]. This study was followed by an intricate *in vivo* comparison of ^{64}Cu-ATSM and ^{18}F-FMISO in tumor-bearing rats with

direct pO_2 tumor measurements, autoradiography and fluorescent microscopy [23]. In rats bearing the R3327-AT rat prostate tumor, there was a poor correlation between the intratumoral distribution of ^{18}F-FMISO and ^{64}Cu-ATSM except at later times (16–20 hr post injection). However, in the same study ^{18}F-FMISO and ^{64}Cu-ATSM images were also acquired in nude rats bearing xenografts derived from the human squamous cell carcinoma cell line, FaDu. For the FaDu tumor model, the early and late ^{64}Cu-ATSM PET images were similar and were in general concordance with the ^{18}F-FMISO scans. Following these discrepancies, a recent publication showed that the ability of Cu-ATSM to delineate hypoxia was suspect primarily in **prostate** tumors in a manner that that was directly related to the expression of fatty acid synthase [24]. It was, therefore, important to continue to validate the use of ^{64}Cu-ATSM against ^{18}F-FMISO in this 9L gliosarcoma model. A previous study compared the autoradiographic distributions of ^{64}Cu-ATSM with a well-established hypoxia marker drug (EF5) in 9L tumors; there was a close correlation between ^{64}Cu- ATSM uptake and hypoxia in 9L tumors [25].

In the current study a comparison was made between the distribution of ^{18}F-FMISO (2 h) and early and late distribution time points for ^{64}Cu-ATSM (10 min and 24 h). Our data show that the distribution of ^{64}Cu-ATSM at both 10 min and 24 h correlates highly with the 2-h distribution of ^{18}F-FMISO. The similarity of the image quality of the radionuclides has been demonstrated (Figure 1A and 1B) and it is, therefore, interesting that the ^{64}Cu-ATSM images show a more focal (localized) distribution of activity. Observed differences in distribution may be attributed to differences in retention mechanisms for the agents and the poor target:background ratios associated with the nitromidazoles. The distribution of ^{64}Cu-ATSM at 24 h does have a greater correlation with ^{18}F-FMISO than the 10 min distribution; however, these differences are not significant and confirm that examination of ^{64}Cu-ATSM at earlier time points is suitable for the delineation of hypoxia within tumors.

4.2. Regional Uptake of ^{64}Cu-ATSM and ^{18}F-FDG Do Not Correlate in 9L Tumors

^{18}F-FDG is utilized widely in many aspects of PET diagnostic medicine, including cancer diagnosis and diseases of the brain and heart. The mechanism of ^{18}F-FDG trapping follows the well-documented glucose biochemical pathway. The direct measurement of glucose metabolism with ^{18}F-FDG also yields valuable information about tumor localization and quantitation. A previous dual-tracer study with ^{64}Cu-ATSM and ^{18}F-FDG in VX2 tumors (implanted into Japanese white rabbits) showed that the major accumulation of ^{64}Cu-ATSM was observed around the outer rim of the tumor masses, which consisted mainly of active hypoxic cells, and ^{18}F-FDG was distributed more widely with highest levels in the inner regions where pre-necrotic cells were mainly observed [26]. An additional study compared the intratumoral distribution of ^{64}Cu-ATSM and ^{18}F-FDG in four mice-tumor models (LLC1, Meth-A, B16 and colon26) with the immunohistochemical staining of proliferating cells (Ki67), blood vessels (CD34 or von Willebrand factor), and apoptotic cells (terminal deoxynucleotidyltransferase-mediated dUTP nick end labeling method) [27]. It was revealed that there are regions within the tumor that contain cells of different phenotypes that can be distinguished by the use of ^{64}Cu-ATSM and ^{18}F-FDG [27].

This current study demonstrates that 9L tumors contain regions of high metabolism that are not very hypoxic and vice versa. It is reasonable and possible for regions of high ^{18}F-FDG uptake to also show both high and low ^{64}Cu-ATSM uptake. Tumor cells in close proximity to the vasculature would presumably have high ^{18}F-FDG uptake, whereas cells remote from the vascular bed could be hypoxic. It is, therefore, possible that both conditions could exist within the same tumor. These data are in agreement with the previously reported animal [27] and clinical data [8–10,12].

4.3. Regional Uptake of ^{64}Cu-ATSM and ^{18}F-FLT Show a Strong Correlation

^{18}F-FLT has been proposed as a PET tracer for cell proliferation [28,29]. It is retained in proliferating cells after phosphorylation by thymidine kinase (TK1). ^{18}F-FLT is taken up by cells and phosphorylated by TK1, which leads to intracellular trapping within the cell. The retention of FLT within the cell provides a measure of cellular TK activity, an enzyme that is closely tied to cellular proliferation. It is apparent that the relationships between proliferation, hypoxia and metabolism are complicated. Studies that compare proliferation with hypoxia markers have led to a wide range of results. In an effort to characterize the distribution of hypoxia and proliferation in human squamous cell carcinoma of the cervix via an immunohistochemical approach, it was shown in 1997 that there was adirect relationship between hypoxia measured by pimonidazole binding and proliferation markers [30]. In a clinical imaging study in 2006, the relationship between ^{18}F-FMISO and tumor markers of hypoxia, proliferation, and angiogenesis showed a weakly positive correlation between both ^{18}F -FMISO ($R^2 = 0.64$) and ^{18}F-FDG uptake ($R^2 = 0.75$) and the proliferative marker Ki67 in peripheral tumor, with no correlation seen in the central tumor [31].

The results in this current study would suggest, at least in the 9L tumor model, that regions of hypoxia as delineated by ^{64}Cu-ATSM also demonstrate increased levels of proliferation as shown by the kinetics of ^{18}F-FLT. This is in contrast to the observation by Tanaka *et al* that abundant positive nuclear staining of Ki67 in tumor cells was observed in the regions of high ^{18}F-FDG uptake, and was hardly observed in regions of ^{64}Cu-ATSM accumulation [27], and, similar to microvessel density, the number of Ki67 positive cells increased with ^{18}F-FDG uptake but decreased with ^{64}Cu-ATSM localization. The reasons for this discrepancy on the macro-level can be related to the fact that hypoxia might develop in different tumors through mechanisms unrelated to oxygen supply. Freyer et al., have demonstrated in spheroids that the oxygen consumption rate may increase as much as 5-fold in cells undergoing active proliferation [32,33]. It has also been shown that angiogenesis occurs in tumors of a very small size (100 cells) [34], and it is reasonable to assume that high oxygen consumption rates in tumors could stimulate angiogenesis by the lowering of pO_2. Moreover, in well-developed tumors, regions with high proliferative rates may create a locoregional hypoxia that is not directly related to the degree of vascularity, perfusion, or oxygen supply.

5. Conclusions

This present study highlights that a number of different situations can exist when considering the complex relationships between regions of high metabolism, proliferation and hypoxia. The 9L tumor exhibits many of the physiological attributes that could be apparent in the clinical situation: tumors with regions of varied metabolism, proliferation and hypoxia which may, or may not, be related to each other but are not discernible due to the resolution restrictions of the imaging modality. Specifically, the 9L tumors contain regions of high metabolism (high FDG uptake) that are not very hypoxic (low Cu-ATSM retention) and *vice versa*. Also seen are regions that demonstrate increased uptake of both tracers and *vice versa*. In regard to proliferation, regional hypoxia within the 9L tumor strongly correlates to increased levels of proliferation as shown by the kinetics of ^{18}F-FLT. It is apparent that Cu-ATSM is a clinically relevant PET agent that has enormous value in the imaging of oncological hypoxia [6–11] and it has clearly been shown with Cu-ATSM that the 9L tumor has regions of hypoxia within its margins. These regions, at the resolution of the autoradiography instrumentation, are also highly proliferative but have varied levels of glucose metabolism.

Acknowledgements

This work was supported by the United States Department of Energy (DE-FG02-87ER60212). The production of copper radionuclides at Washington University is supported by a grant from the National Cancer Institute (1 R24

CA86307). We wish to thank Debbie Sultan, Todd Perkins and Thomas Voller for production of ^{64}Cu, John Engelbach, and Lynne Jones for technical assistance, and Bill Margenau for cyclotron support. We also thank Dr. Joseph B. Dence for his editing of this manuscript.

This work was supported by a grant from the U. S. Department of Energy (Grant DE FG02-87ER60512). The production of copper radionuclides at Washington University is supported by a grant from the National Cancer Institute (Grant 1 R24 CA86307).

REFERENCES

1. Tatum JL, Kelloff GJ, Gillies RJ, Arbeit JM, Brown JM, Chao KSC, Chapman JD, Eckelman WC, Fyles AW, Giaccia AJ, Hill RP, Koch CJ, Krishna MC, Krohn KA, Lewis JS, Mason RP, Melillo G, Padhani AR, Powis G, Rajendran JG, Reba R, Robinson SP, Semenza GL, Swartz HM, Vaupel P, Yang D, Croft B, Hoffman J, Liu G, Stone H, Sullivan D. Hypoxia: Importance in tumor biology, noninvasive measurement by imaging, and value of its measurement in the management of cancer therapy. Int J Radiat Biol 2006;82:699–757. [PubMed: 17118889]
2. Brown JM. The hypoxic cell: A target for selective cancer therapy-Eighteenth Bruce F. Cain Memorial Award Lecture. Cancer Res 1999;59:5863–5870. [PubMed: 10606224]
3. Graeber TG, Osmanian C, Jacks T, Housman DE, Koch CJ, Lowe SW, Giaccia AJ. Hypoxia-mediated selection of cells with diminished apoptotic potential in solid tumours. Nature (Lond) 1996;379:88–91. [PubMed: 8538748]
4. Höckel M, Schlenger K, Aral B, Mitze M, Schäffer U, Vaupel P. Association between tumor hypoxia and malignant progression in advanced cancer of the uterine cervix. Cancer Res 1996;56:4509–4515. [PubMed: 8813149]
5. Shweiki D, Itin A, Soffer D, Keshet E. Vascular endothelial growth factor induced by hypoxia may mediate hypoxia-initiated angiogenesis. Nature (Lond) 1992;359:843–845. [PubMed: 1279431]
6. Vavere AL, Lewis JS. Cu-ATSM: A radiopharmaceutical for the PET imaging of hypoxia. Dalton Trans 2007;43:4893–4902. [PubMed: 17992274]
7. Fujibayashi Y, Taniuchi H, Yonekura Y, Ohtani H, Konishi J, Yokoyama A. Copper-62-ATSM: A new hypoxia imaging agent with high membrane permeability and low redox potential. J Nucl Med 1997;38:1155–1160. [PubMed: 9225812]
8. Dehdashti F, Grigsby PW, Lewis JS, Laforest R, Siegel BA, Welch MJ. Assessing tumor hypoxia in cervical cancer by positron emission tomography with ^{60}Cu-ATSM. J Nucl Med 2008;49:201–205. [PubMed: 18199612]
9. Dehdashti F, Grigsby PW, Mintun MA, Lewis JS, Siegel BA, Welch MJ. Assessing tumor hypoxia in cervical cancer by positron emission tomography with ^{60}Cu-ATSM: relationship to therapeutic response - a preliminary report. Int J Radiat Biol Phys 2003;55:1233–1238.
10. Dehdashti F, Mintun MA, Lewis JS, Bradley J, Govindan R, Laforest R, Welch MJ, Siegel BA. In vivo assessment of tumor hypoxia in lung cancer with ^{60}Cu-ATSM. Eur J Nucl Med Mol Imaging 2003;30:844–850. [PubMed: 12692685]
11. Dietz DW, Dehdashti FD, Grigsby PW, Malyapa RS, Myerson RJ, Picus J, Ritter J, Lewis JS, Welch MJ, Siegel BA. Tumor hypoxia detected by Positron Emission Tomography with ^{60}Cu-ATSM as a predictor of response and survival in patients undergoing neoadjuvant chemoradiotherapy for rectal carcinoma: a pilot study. Dis Colon Rec. 2008in press
12. Rajendran JG, Mankoff DA, O'Sullivan F, Peterson LM, Schwartz DL, Conrad EU, Spence AM, Muzi M, Farwell DG, Krohn KA. Hypoxia and glucose metabolism in malignant tumors: Evaluation by [^{18}F]fluoromisonidazole and [^{18}F]fluorodeoxyglucose positron emission tomography imaging. Clin Cancer Res 2004;10:2245–2252. [PubMed: 15073099]
13. Okada J, Yoshikawa K, Itami M, Imaseki K, Uno K, Itami J, Kuyama J, Mikata A, Arimizu N. Positron emission tomography using fluorine-18-fluorodeoxyglucose in malignant lymphoma: a comparison with proliferative activity. J Nucl Med 1992;33:325–329. [PubMed: 1740697]
14. Vesselle H, Schmidt RA, Pugsley JM, Li M, Kohlmyer SG, Vallières E, E WD. Lung cancer proliferation correlates with [F-18]fluorodeoxyglucose uptake by positron emission tomography. Clin Cancer Res 2000;6:3837–3844. [PubMed: 11051227]

15. Buck AK, Halter G, Schirrmeister H, Kotzerke J, Wurziger I, Glatting G, Mattfeldt T, Neumaier B, Reske SN, Hetzel M. Imaging proliferation in lung tumors with PET: ^{18}F-FLT Versus ^{18}F-FDG. J Nucl Med 2003;44:1426–1431. [PubMed: 12960187]
16. Fujibayashi Y, Taniuchi H, Yonekura Y, Ohtani H, Konishi J, Yokoyama A. Copper-62-ATSM: A new hypoxia imaging agent with high membrane permeability and low redox potential. J Nucl Med 1997;38:1155–1160. [PubMed: 9225812]
17. McCarthy TJ, Dence CS, Welch MJ. Application of microwave heating to the synthesis of [^{18}F] fluoromisonidazole. Appl Radiat Isot 1993;44:1129–1132. [PubMed: 8358401]
18. Machulla HJ, Blocher A, Kuntzsch M, Piert M, Wei R, Grierson JR. Simplified labeling approach for synthesizing 3'-deoxy-3'-[^{18}F]fluorothymidine ([^{18}F]FLT). J Radioanal Nucl Chem 2000;243:843–846.
19. Tai Y-C, Ruangma A, Rowland D, Siegel S, Newport DF, Chow PL, Laforest R. Performance evaluation of the microPET Focus: A third-generation microPET scanner dedicated to animal imaging. J Nucl Med 2005;46:455–463. [PubMed: 15750159]
20. Nunn A, Linder K, Strauss HW. Nitroimidazoles and imaging hypoxia. Eur J Nucl Med 1995;22:265–280. [PubMed: 7789400]
21. Rajendran JG, Wilson DC, Conrad EU, Peterson LM, Bruckner JD, Rasey JS, Chin LK, Hofstrand PD, Grierson JR, Eary JF, Krohn KA. [^{18}F]FMISO and [^{18}F]FDG PET imaging in soft tissue sarcomas: correlation of hypoxia, metabolism and VEGF expression. Eur J Nucl Med Mol Imaging 2003;30:695–704. [PubMed: 12632200]
22. Burgman P, O'Donoghue JA, Lewis JS, Welch MJ, Humm JL, Ling CC. Cell line dependent differences in uptake and retention of the hypoxia selective nuclear imaging agent Cu-diacetyl-bis (N^4-methylthiosemicarbazone) (Cu-ATSM). Nucl Med Biol 2005;32:623–630. [PubMed: 16026709]
23. O'Donoghue JA, Zanzonico P, Pugachev A, Wen B, Smith-Jones P, Cai S, Burnazi E, Finn RD, Burgman P, Ruan S, Lewis JS, Welch MJ, Ling CC, Humm JL. Assessment of regional tumor hypoxia using ^{18}F-fluoromisonidazole and ^{64}Cu(II)-diacetyl-bis(N^4-methylthiosemicarbazone) positron emission tomography: Comparative study featuring microPET imaging, pO_2 probe measurement, autoradiography, and fluorescent microscopy in the R3327-AT and FaDu rat tumor models. Int J Radiat Onc Biol Phys 2005;61:1493–1502.
24. Vavere AL, Lewis JS. Examining the relationship between Cu-ATSM hypoxia selectivity and fatty acid synthase expression in human prostate cancer cell lines. 2008. Nucl Med Biol 2008;35:273–279. [PubMed: 18355682]
25. Yuan H, Schroeder T, Bowsher JE, Hedlund LW, Wong T, Dewhirst MW. Intertumoral differences in hypoxia selectivity of the PET imaging agent ^{64}Cu(II)-diacetyl-bis(N_4-methylthiosemicarbazone). J Nucl Med 2006;47:989–998. [PubMed: 16741309]
26. Obata A, Yoshimoto M, Kasamatsu S, Naiki H, Takamatsu S, Kashikura K, Furukawa T, Lewis JS, Welch MJ, Saji H, Yonekura Y, Fujibayashi Y. Intratumoral distribution of ^{64}Cu-ATSM: a comparison study with FDG. Nucl Med Biol 2003;30:529–534. [PubMed: 12831991]
27. Tanaka T, Furukawa T, Fujieda S, Kasamatsu S, Yonekura Y, Fujibayashi Y. Double-tracer autoradiography with Cu-ATSM/FDG and immunohistochemical interpretation in four different mouse implanted tumor models. Nucl Med Biol 2006;33:743–750. [PubMed: 16934693]
28. Shields AF, Grierson JR, Dohmen BM, Machulla HJ, Stayanoff JC, Lawhorn-Crews JM, Obradovich JE, Muzik O, Mangner TJ. Imaging proliferation in vivo with [F-18]FLT and positron emission tomography. Nature Med 1998;4:1334–1336. [PubMed: 9809561]
29. Shields AF, Grierson JR, Stayanoff JC, Lawhorn-Crews JM, Obradovich J, Muzik O, Mangner T. [F-18] FLT can be used to image cell proliferation in vivo. J Nucl Med 1998;39:228p–228p. [PubMed: 9476923]
30. Kennedy AS, Raleigh JA, Perez GM, Calkins DP, Thrall DE, Novotny DB, Varia MA. Proliferation and hypoxia in human squamous cell carcinoma of the cervix: first report of combined immunohistochemical assays. Int J Radiat Onc Biol Phys 1997;37:897–905.
31. Cherk MH, Foo SS, Poon AMT, Knight SR, Murone C, Papenfuss AT, Sachinidis JI, Saunder THC, O'Keefe GJ, Scott AM. Lack of correlation of hypoxic cell fraction and angiogenesis with glucose

metabolic rate in non-small cell lung cancer assessed by ^{18}F-fluoromisonidazole and ^{18}F-FDG PET. J Nucl Med 2006;47:1921–1926. [PubMed: 17138734]

32. Freyer JP. Rates of oxygen consumption for proliferating and quiescent cells isolated from multicellular tumor spheroids. Adv Exp Med Biol 1994;345:335–342. [PubMed: 8079727]
33. Freyer JP, Sutherland RM. A reduction in the in situ rates of oxygen and glucose consumption of cells in EMT6/Ro spheroids during growth. J Cell Physiol 1985;124:516–524. [PubMed: 4044662]
34. Li C-Y, Shan S, Huang Q, Braun RD, Lanzen J, Hu K, Lin P, Dewhirst MW. Initial stages of tumor cell-induced angiogenesis: Evaluation via skin window chambers in rodent models. J Natl Cancer Institute 2000;92:143–147.

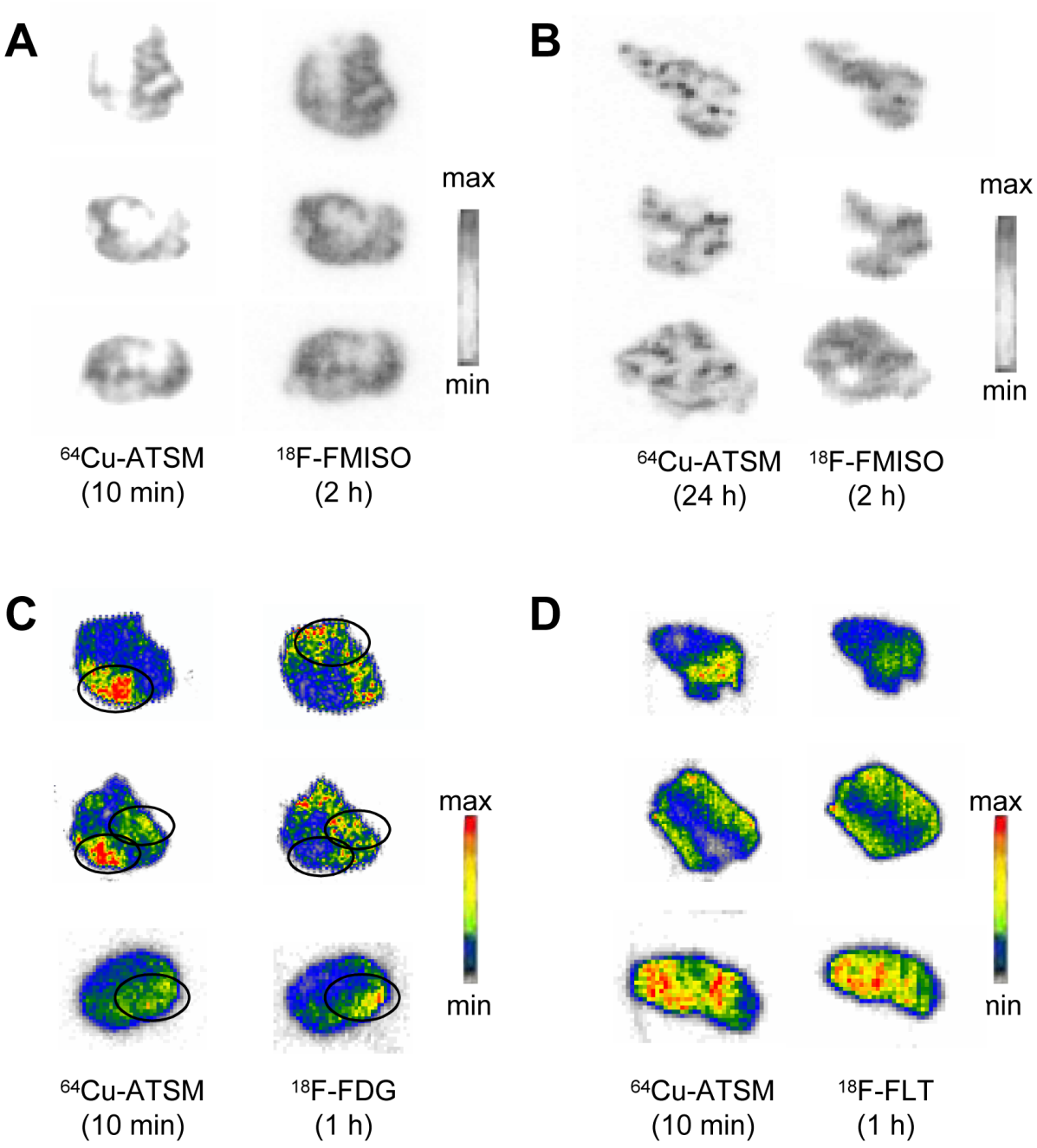

Fig. 1.

Ex vivo electronic autoradiographs of the regional *in vivo* uptake of (A, B) ^{18}F-FMISO, (C) ^{18}F-FDG, (D) ^{18}F-FLT with ^{64}Cu(ATSM) in 9L gliosarcomas. The images shown are representative of the typical dual-tracer autoradiographs obtained from all of the slices of the 9L tumors from rats. Shown in each panel are three representative slices chosen at random from a total of 120 slices from 5 tumors. Shown are slices with following ^{18}F tracer collection (right) and the ^{64}Cu-ATSM distribution (left) in the *same* tumor slices. At the time of imaging, the ^{18}F images are generated 99% by ^{18}F. Following 24 h decay the images are generated from 95+% ^{64}Cu.

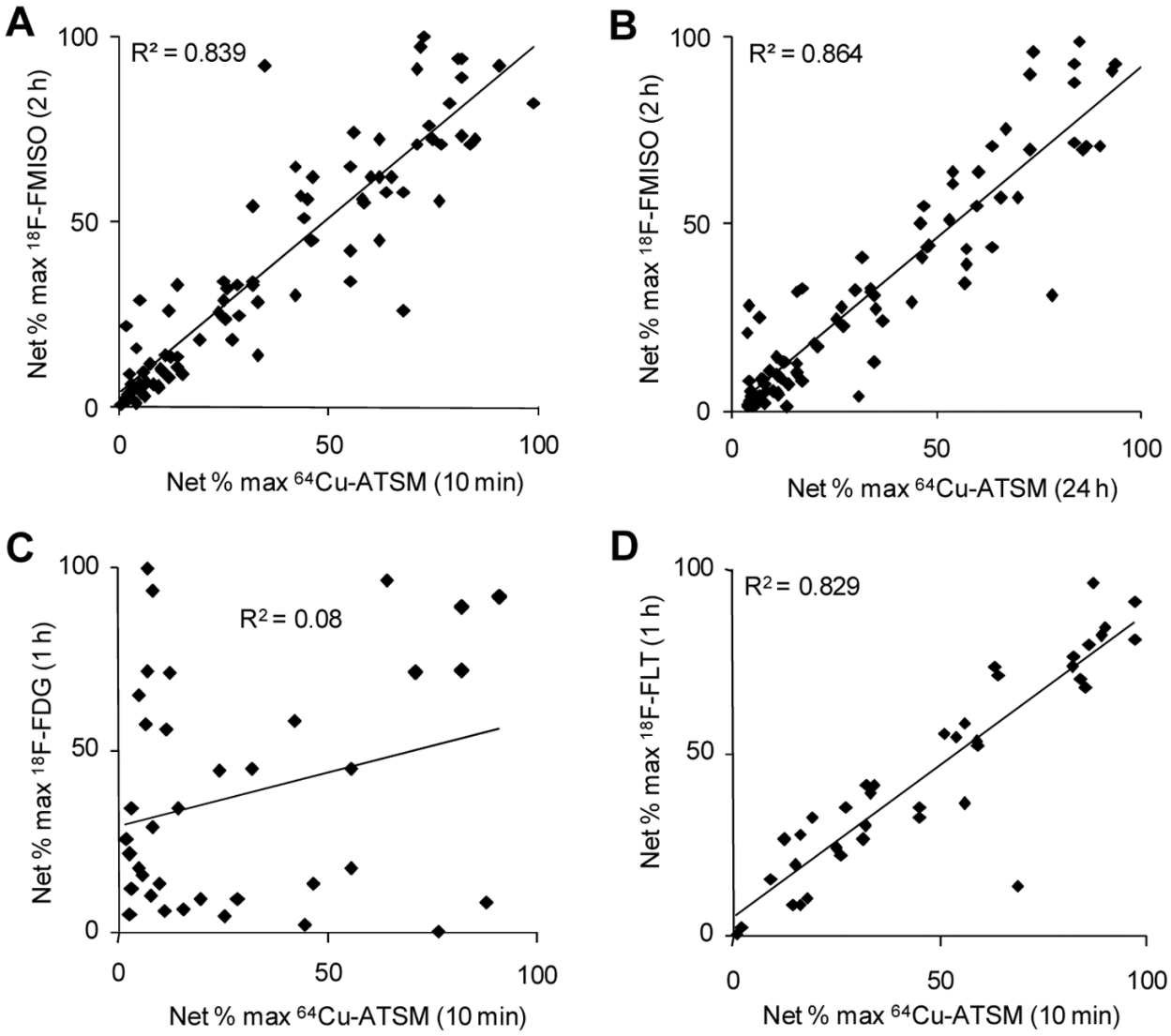

Fig. 2.

A direct measurement of the regional uptake of the ^{18}F-agents and ^{64}Cu-ATSM in 9L tumors. The correlation is based on the direct measurement of the net % maximum uptake (cpm) of the ^{18}F agent and ^{64}Cu-ATSM by use of software supplied with the Packard InstantImager. A significant correlation is seen between the regional uptake following ^{18}F-FMISO (2 h distribution) and ^{64}Cu-ATSM at (A) 10 min distribution and (B) 24 h distribution. No correlation is seen between the regional uptake following (C) ^{18}F-FDG (1 h) and ^{64}Cu-ATSM (10 min), but a significant correlation is observed between the distribution of (D) ^{18}F-FLT (1 h) and ^{64}Cu-ATSM (10 min).

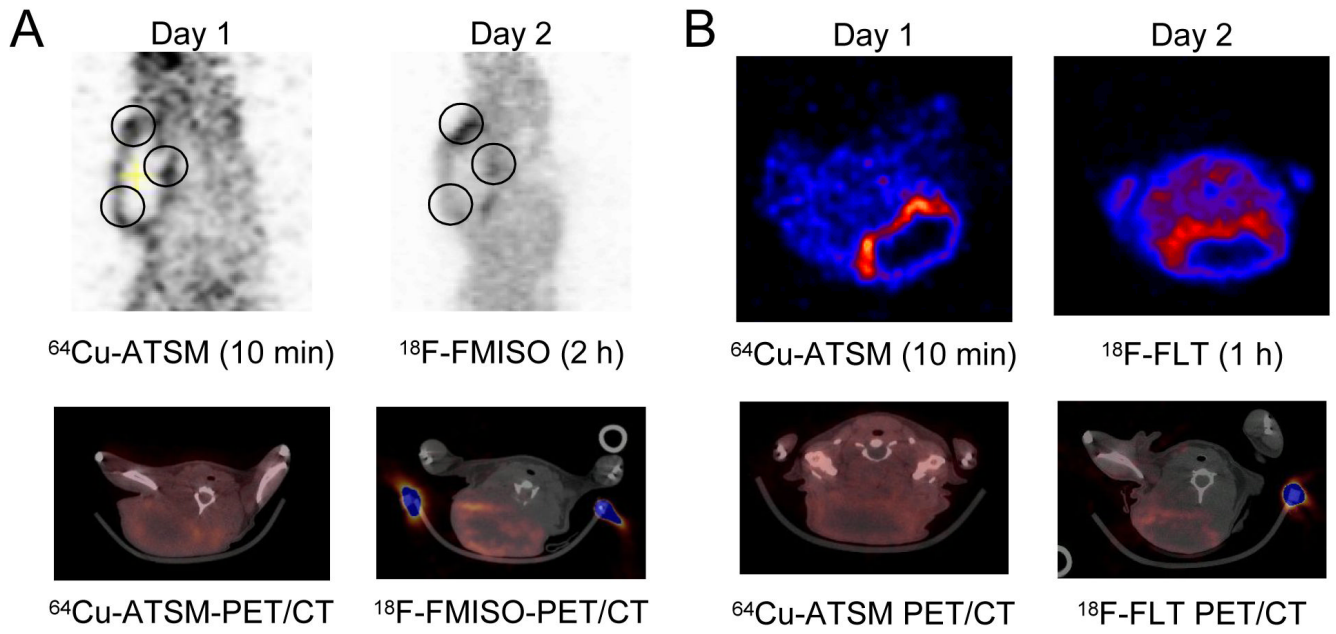

Fig. 3.

Representative PET images from ^{18}F-FMISO or ^{18}F-FLT and ^{64}Cu-ATSM imaging in the same animals. On Day 1, 150 μCi ^{64}Cu-ATSM was injected into the animals and imaged on the microPET-FOCUS 10 min post-injection; then on Day 1, the same animals were injected with 1.5 mCi of the respective ^{18}F-FLT compound and reimaged at the required time point. (A) Sagittal PET images comparing the distribution of 10 min ^{64}Cu-ATSM distribution with 2 h ^{18}F-FMISO in the same tumor slice. Black circles denote similar regions of uptake, with a clearer delineation of regional uptake in the ^{64}Cu-ATSM image. Below are representative transaxial PET/CT slices through the same point in the tumor. Histology confirmed a necrotic center to the tumor. (B) Transaxial PET images that compare the distribution of 10 min ^{64}Cu-ATSM distribution with 1 h ^{18}F-FLT in the same tumor slice. Below are representative transaxial PET/CT slices through the same point in the tumor. Histology confirmed a necrotic center to the tumor.